A causative link between the structure of aberrant protein oligomers and their toxicity

nature chemical biology

ARTICLE

PUBLISHED ONLINE: 10 JANUARY 2010 | DOI: 10.1038/NCHEMBIO.283

A causative link between the structure of aberrant protein oligomers and their toxicity

Silvia Campioni[1,4], Benedetta Mannini[1], Mariagioia Zampagni[1], Anna Pensalfini[1,4], Claudia Parrini[2], Elisa Evangelisti[1], Annalisa Relini[2], Massimo Stefani[1], Christopher M Dobson[3], Cristina Cecchi[1] & Fabrizio Chiti[1]*

The aberrant assembly of peptides and proteins into fibrillar aggregates proceeds through oligomeric intermediates that are thought to be the primary pathogenic species in many protein deposition diseases. We describe two types of oligomers formed by the HypF-N protein that are morphologically and tinctorially similar, as detected with atomic force microscopy and thioflavin T assays, though one is benign when added to cell cultures whereas the other is toxic. Structural investigation at a residue-specific level using site-directed labeling with pyrene indicated differences in the packing of the hydrophobic interactions between adjacent protein molecules in the oligomers. The lower degree of hydrophobic packing was found to correlate with a higher ability to penetrate the cell membrane and cause an influx of Ca^{2+} ions. Our findings suggest that structural flexibility and hydrophobic exposure are primary determinants of the ability of oligomeric assemblies to cause cellular dysfunction and its consequences, such as neurodegeneration.

The accumulation of specific peptides or proteins as misfolded extracellular amyloid fibrils or structurally related intracellular inclusions is the hallmark of over 40 human pathologies, ranging from neurodegenerative disorders (such as, Alzheimer's, Parkinson's and prion diseases) to non-neuropathic systemic amyloidoses (for example, dialysis-related amyloidosis and light chain amyloidosis) and localized amyloidoses (such as type II diabetes and atrial amyloidosis)[1]. It is increasingly evident that, at least in some protein deposition diseases, the pathogenic species are the oligomeric assemblies that precede the formation of mature amyloid fibrils[2–8]. A structural characterization of the oligomers directed to an understanding of the relationship between their structural characteristics and their toxic effects is difficult to achieve, mainly because these species are typically transient and structurally heterogeneous, thus considerably hampering their investigation. As a consequence, the structural determinants of the protein oligomers that are responsible for cell dysfunction are not yet clear.

The small, 91-residue N-terminal domain of *Escherichia coli* HypF (HypF-N) is a stably folded α/β protein with a ferredoxin-like fold[9]. HypF-N is a valuable model system for investigating the structural basis of the cellular dysfunction caused by misfolded protein oligomers. First, monomeric HypF-N is readily able to form spherical oligomers, protofibrils and amyloid-like fibrils *in vitro*, under conditions that destabilize its native state or promote its co-operative unfolding into partially structured species[10–12]. Second, the oligomers that form in the early stages of the aggregation process have the same morphological, structural and tinctorial features as those formed by disease-related peptides and proteins[11,12], and they impair cell viability when added to the extracellular medium of cultured cells[13,14] and when injected into rat brains[15]. Finally, and most importantly in the context of the present study, HypF-N can rapidly be converted into oligomers that remain populated persistently, rather than transiently, and are sufficiently stable to maintain their structure and properties even when transferred to conditions that are very different from those that promote their formation.

In this paper we report the finding that two types of stable oligomers can be formed *in vitro* from HypF-N that are apparently indistinguishable on the basis of thioflavin T (ThT) binding and display very similar morphologies when inspected by atomic force microscopy (AFM), but that differ in that one induces cellular dysfunction whereas the other is benign. This observation not only demonstrates that aggregates with similar morphology can have different biological properties, but also provides a unique opportunity to investigate the structural determinants of oligomer toxicity through comparative studies of their properties. By using protein engineering and structural mapping by means of *N*-(1-pyrene)maleimide (PM) labeling and detection of excimer formation, we have identified the specific regions of the sequence that are structured in the toxic and nontoxic oligomers, determined the major differences between them, and addressed the relationship between oligomer structure and cellular impairment.

RESULTS

Morphologically similar oligomers show different toxicity

In order to obtain two types of stable oligomeric species, we incubated HypF-N for 4 h at 48 μM, 25 °C in (i) 50 mM acetate buffer, 12% (v/v) trifluoroethanol (TFE), 2 mM DTT, pH 5.5 (condition A) and (ii) 20 mM trifluoroacetic acid (TFA), 330 mM NaCl, pH 1.7 (condition B). The oligomers were then resuspended in a physiological medium at pH 7.0 with no added co-solvent. Tapping-mode AFM (TM-AFM) images revealed the presence of spherical bead-like aggregates with heights in the range of 2–6 nm and 2–7 nm under conditions A (**Fig. 1a**) and B (**Fig. 1b**), respectively. ThT binding assays showed that both types of oligomers bind this amyloid-specific dye and increase its fluorescence to similar extents, indicating the presence of extensive intermolecular β-sheet structure (**Supplementary Results** and **Supplementary Fig. 1**).

[1]Department of Biochemical Sciences, University of Florence, Florence, Italy. [2]Department of Physics, University of Genoa, Genoa, Italy. [3]Department of Chemistry, University of Cambridge, Cambridge, UK. [4]Present addresses: Department of Chemistry and Applied Biosciences, Laboratory of Physical Chemistry, Eidgenössische Technische Hochschule Zürich, Zurich, Switzerland (S.C.), and Department of Molecular Biology and Biochemistry, University of California, Irvine, California, USA (A.P.). *e-mail: fabrizio.chiti@unifi.it

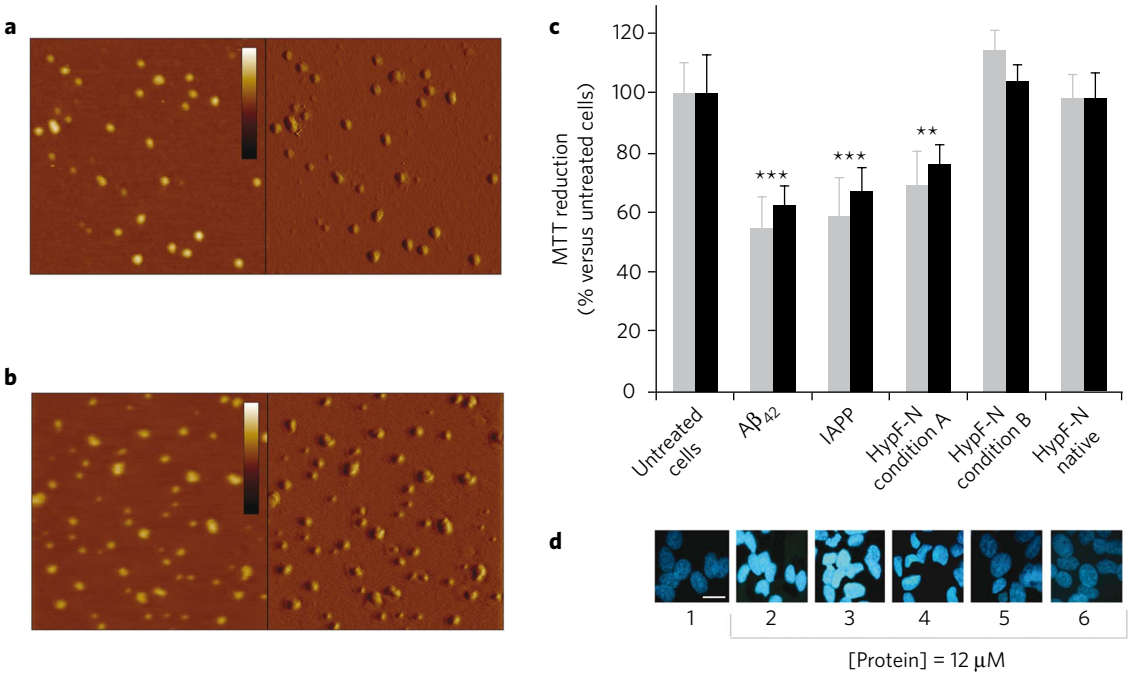

Figure 1 | Morphology and toxicity of HypF-N aggregates. (**a**,**b**) TM-AFM images (left, height data; right, amplitude data) of HypF-N samples pre-incubated under conditions A (**a**) and B (**b**) and then resuspended at pH 7.0. Scan size, 500 nm. The color bar corresponds to a *Z* range of 7 nm. (**c**) MTT reduction assay on SH-SY5Y (gray) and Hend (black) cells untreated (lane 1) or treated with $A\beta_{42}$ oligomers (lane 2), IAPP oligomers (lane 3), HypF-N aggregates formed under condition A (lane 4) and B (lane 5), and native HypF-N (lane 6). Error bars correspond to the s.d. values of four independent experiments. Double and triple asterisks refer to *P* values lower than 0.01 and 0.001, respectively. (**d**) Hoechst staining of SH-SY5Y cells untreated (image 1) or treated with $A\beta_{42}$ oligomers (image 2), IAPP oligomers (image 3), HypF-N aggregates formed under condition A (image 4) and B (image 5) and native HypF-N (image 6). The protein concentration reported refers to monomer concentrations. All images have been acquired at the same magnification. The scale bar represents 20 μm.

These species did not resolubilize when placed under physiological conditions, as indicated by the preservation of their ability to bind ThT (**Supplementary Fig. 1**). Moreover, neither type of oligomer underwent any detectable structural reorganization following such a change of the medium (see below).

To assess the biological activity of the spherical aggregates formed under conditions A and B, we transferred the aggregates to physiological conditions and added them to the cell culture media of human neuroblastoma cells (SH-SY5Y) and mouse endothelial cells (Hend). The state of the cells was first monitored, in each case, by performing the 3-(4,5-dimethylthiazol-2-yl)-2,5-diphenyltetrazolium bromide (MTT) reduction inhibition assay—a generic biochemical test used to monitor cell viability[16]. The aggregates formed under condition A were found to decrease MTT reduction substantially, relative to untreated cells, in both cell lines (**Fig. 1c**). Indeed, their effect is comparable to that of the oligomers formed by $A\beta_{42}$ and IAPP (associated with Alzheimer's disease and type II diabetes, respectively), which were used here as positive controls[17,18]. By contrast, the aggregates formed under condition B had essentially no effect on the ability of either SH-SY5Y or Hend cells to reduce MTT (**Fig. 1c**). No inhibition of MTT reduction was observed when the cells were treated with native HypF-N (**Fig. 1c**).

We also stained SH-SY5Y cells with the apoptotic marker Hoechst 33342, which binds to the highly condensed chromatin present in the nuclei of apoptotic cells, giving rise to a strong fluorescence signal and allowing the visualization of abnormal nuclei[18,19]. Fluorescence microscopy images indicate that the nuclei of the cells treated with HypF-N aggregates formed under condition A were prominently stained with this dye and often appeared abnormal in shape (**Fig. 1d**), to an extent similar to that of the cells treated with $A\beta_{42}$ and IAPP aggregates (**Fig. 1d**). By contrast, the nuclei of cells treated with the aggregates formed under condition B or with the native protein exhibited a much lower degree of staining, similar to that of untreated cells (**Fig. 1d**). Control experiments indicated that the lack of toxicity of the species formed under condition B is not due to an insufficient quantity of oligomeric aggregates present in the experiments (**Supplementary Fig. 2**). Taken together, these results indicate that the same polypeptide sequence can assemble into two distinct types of stable oligomers having similar morphological and tinctorial properties, but different abilities to cause cellular dysfunction.

Structural core of the nontoxic HypF-N oligomers

To gain insight into the structural differences of the two types of oligomers, we expressed 18 mutational variants of the protein, each carrying a single cysteine residue but located at different positions along the polypeptide chain, and labeled them with PM. Each labeled variant was then allowed to aggregate separately under the different conditions, and the fluorescence spectra of the resulting samples were acquired and analyzed. PM is a probe of the proximity between pairs of labeled residues in the species under investigation, because of its ability to form excited-state dimers, or excimers, when two PM moieties are within a short distance (about 10 Å) of each other[20–22]. Excimer formation gives rise to a band in the 430–470 nm region of the PM fluorescence emission spectrum[20–22]; the presence or absence of this band therefore allows us to determine whether a labeled position is close (≤10 Å) or distant (>10 Å), respectively, to the same labeled position in an adjacent protein molecule in the oligomer[21,22]. One caveat is that the PM moieties have the potential to perturb the aggregation process; this potential problem is, however, avoided in our comparative experiments, as discussed below.

The fluorescence emission spectra of samples containing HypF-N labeled with PM at residues 5, 10, 18 and 47 and incubated

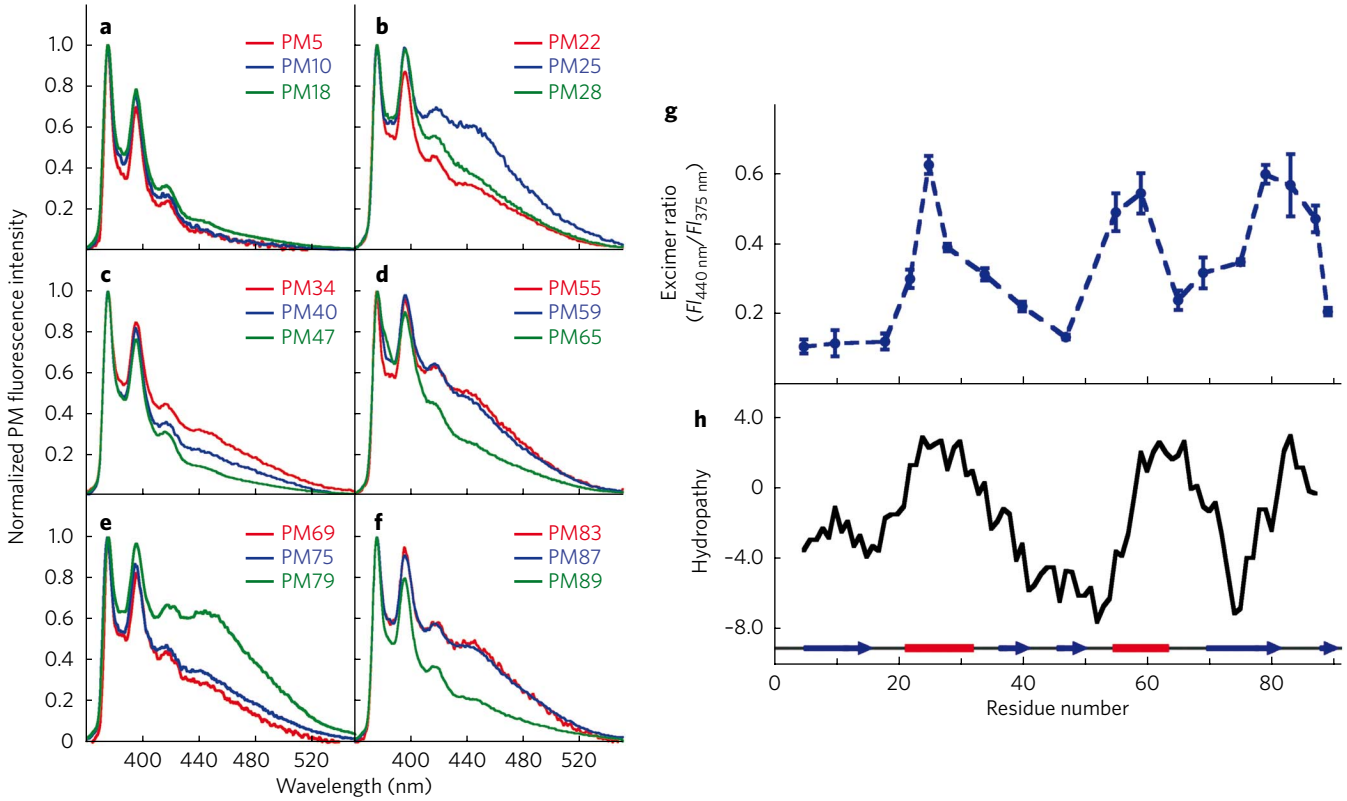

Figure 2 | Structural properties of the oligomers formed under condition B. (**a**–**f**) Fluorescence emission spectra of HypF-N oligomers formed under condition B by protein chains labeled with PM at different positions. Spectra were acquired at 48 μM protein. The color code reported in each panel helps associate the spectrum with the position of PM labeling. Spectra have been normalized to the intensity of the peak centered at 375 nm. (**g**) Ratio between the fluorescence intensities measured at 440 nm (excimer peak) and 375 nm (monomer peak) for all the labeled positions along the HypF-N sequence. Error bars correspond to s.d. of at least two independent experiments per position. (**h**) Hydropathy profile of HypF-N calculated using the Roseman hydrophobicity scale[44]. The positions of α-helices (red) and β-strands (blue) in the native structure (Protein Data Bank entry 1GXU) are also indicated as determined by MOLMOL[45].

under condition B did not feature an excimer component in the 430–470 nm region (**Fig. 2a**–**f**). In all other cases an excimer peak centered at about 440 nm was detected in the fluorescence spectrum; this peak was, however, of low intensity for protein variants labeled at residues 22, 28, 34, 40, 65, 69, 75 and 89, but of higher intensity when residues 25, 55, 59, 79, 83 and 87 were labeled (**Fig. 2a**–**f**). These results indicate that for the first group of variants, those exhibiting no excimer band, the distance between the labeled residues in adjacent molecules is greater than 10 Å. For the second group of variants, with weak excimer bands, the labeled residues are at intermediate distances from each other in the oligomers, or alternatively in close proximity in only a fraction of the oligomers that are present in solution. Finally, for the third group of variants, those with strong excimer bands, the labeled residues are in close proximity (≤ 10 Å) to the same residue on one or more adjacent molecules and indeed are likely to adopt well-defined structure.

From such data we were able to calculate the ratio of the excimer-to-monomer fluorescence intensities (FI_{440nm}/FI_{375nm}) for each labeled residue (**Fig. 2g**). The profile of excimer ratio versus residue number suggests that the regions spanning approximately residues 22–34, 55–59 and 75–87 form the structural core of the HypF-N oligomers formed under condition B, as the residues in these regions of the sequence have a high tendency to be in close proximity with the corresponding residues of adjacent molecules within the oligomers. The excimer ratio data do not rule out the possibility that the residues within these regions are also in close proximity with residues located in other portions of the protein chain (see below). Nevertheless, they clearly indicate that specific regions of the molecule are tightly packed within the structural core of these HypF-N oligomers. Notably, there is excellent agreement between the locations of these three regions (**Fig. 2g**) and the three major peaks in the hydropathy profile of HypF-N (**Fig. 2h**); our data indicate, therefore, that the regions of the sequence with the highest hydrophobicity contribute to the structural core of the nontoxic aggregates formed by HypF-N.

The core of the toxic oligomers is less tightly packed

The same approach was then used to gain insight into the structure of the toxic aggregates formed under condition A (**Fig. 3a**–**f**). For these species, molecules labeled at residues 5, 10, 34, 40, 47 and 89 had no significant excimer components in the spectra (**Fig. 3a**,**c**,**f**). By contrast, all the remaining positions (18, 22, 25, 28, 55, 59, 65, 69, 75, 79, 83 and 87) showed faint excimer peaks (**Fig. 3a**–**f**). None of the labeled variants gave rise to spectra with intense excimer bands (**Fig. 3a**–**f**), indicating that in no case do adjacent molecules pack together such that their corresponding residues are persistently in close proximity. A comparison between the values of the excimer ratios obtained for the toxic and nontoxic aggregates is reported in **Figure 3g**. The major differences involve the three hydrophobic regions of the sequence that yield high values of excimer ratio in the nontoxic aggregates and much smaller values in the toxic ones (**Fig. 3g**). Differences between the values of excimer ratio in the other regions are either insignificant or, at most, subtle (**Fig. 3g**). This finding indicates that the degree of ordered intermolecular packing between corresponding hydrophobic regions of adjacent HypF-N molecules is less marked in the case of the toxic aggregates.

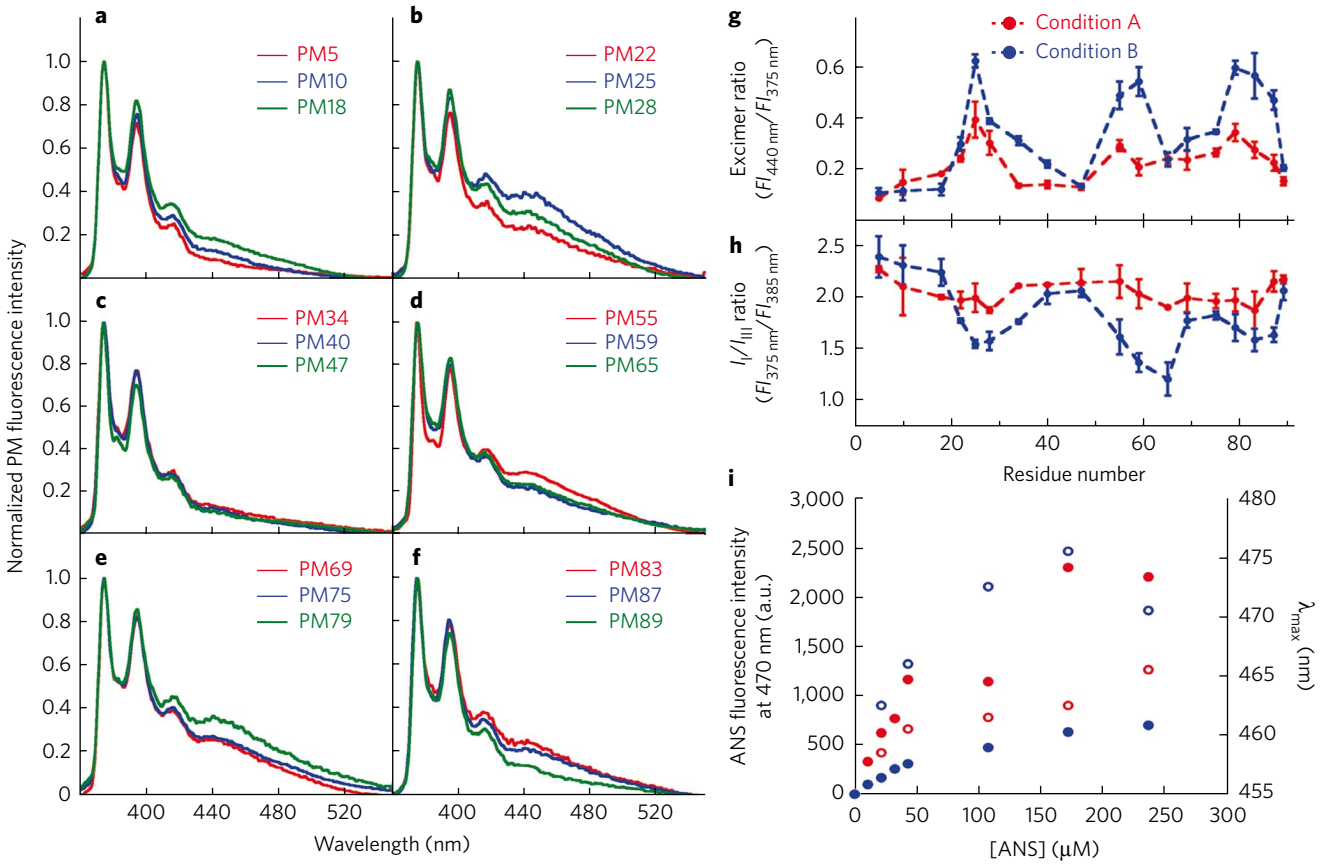

Figure 3 | Structural properties of the oligomers formed under condition A. (**a**–**f**) Fluorescence emission spectra of HypF-N oligomers formed under condition A by protein chains labeled with PM at different positions. Spectra were acquired at 48 μM protein. The color code reported in each panel helps associate the spectrum with the position of PM labeling. (**g**) Excimer ratio profiles of HypF-N oligomers formed under conditions A (red) and B (blue). Error bars correspond to s.d. of at least two independent experiments per position. (**h**) Ratio between the fluorescence intensities measured at 375 nm (I_I) and 385 nm (I_{III}) for all the labeled positions along the HypF-N sequence. Error bars correspond to s.d. of at least two independent experiments. Low and high ratio values correspond to a nonpolar and highly polar environment, respectively[23]. Values of 2.78 and 2.03 were obtained for glutathione labeled with PM and dissolved in water and 1-octanol, respectively (**Supplementary Fig. 4**). Our values are higher than those previously reported for free pyrene[23]. Similar values have also been obtained by other authors[24–26] and are due to the fact that pyrene is conjugated to a polypeptide chain through a maleimide moiety rather than being free in solution. (**i**) ANS binding to HypF-N oligomers formed under condition A (red) and B (blue). The ANS fluorescence intensity measured at 470 nm (filled circles) and the wavelength of maximum emission (λ_{max}, empty circles) are reported as a function of the ANS concentration. Protein concentration was 43 μM in all cases.

We also recorded the fluorescence emission spectra of 1:1 mixtures of aggregates labeled with PM at different positions (25, 55, 59, 83, 87), prepared under both conditions A and B (**Supplementary Fig. 3a**,**b**). At least in some cases, distinct positions from adjacent molecules appeared to be spatially close as they gave rise to a medium or strong excimer signal. However, the excimer ratio values obtained for the toxic oligomers were considerably lower than those of the nontoxic oligomers.

To obtain information on the polarity of the environment explored by the PM moieties in the oligomers formed under conditions A and B, we calculated the ratio of the fluorescence intensities at 375 nm (I_I) and 385 nm (I_{III}) for all the labeled positions along the HypF-N sequence[23]. A value of 2.78 was obtained for the I_I/I_{III} ratio for a fully soluble and unstructured PM-labeled glutathione dissolved in water (**Supplementary Fig. 4**). This value is in agreement with that reported elsewhere for a fully solvent-exposed PM conjugated to proteins[24–26] and represents an upper bound for our measurements. The I_I/I_{III} values obtained for the two types of HypF-N aggregates indicate that the PM moieties are more accessible to the solvent (higher I_I/I_{III} ratios) in the toxic oligomers formed under condition A than in the nontoxic oligomers formed under condition B, particularly at the level of the three major hydrophobic regions (**Fig. 3h**). Moreover, in the case of the oligomers formed under condition B, there is a good agreement between the labeled positions found to be buried into a nonpolar environment and the regions of the sequence that form the structural core of the aggregates—that is, 22–34, 55–59 and 75–87 (**Fig. 3g**,**h**). Overall, the results of the excimer and I_I/I_{III} ratio values indicate that in the toxic oligomers, the hydrophobic regions are structurally more highly disorganized and solvent-exposed than they are in the nontoxic oligomers.

The structural differences do not arise from artifacts

In order to interpret the data reported here, it is important to address the possibility that the PM moieties perturb in some manner the aggregation behavior of HypF-N in one or both of the conditions in which these studies were carried out. TM-AFM images obtained for HypF-N samples labeled at positions 10 and 59 and left to aggregate under conditions A and B showed that the globular morphology of the aggregates is preserved upon labeling (**Supplementary Fig. 5**). Moreover, both types of HypF-N oligomers labeled at positions 10, 25, 47 and 59 retained the ability to bind ThT (**Supplementary Fig. 6a**).

In more structural detail, our analysis is comparative and aims to explore any significant structural differences between the two types of aggregates; the differences revealed in the values of excimer

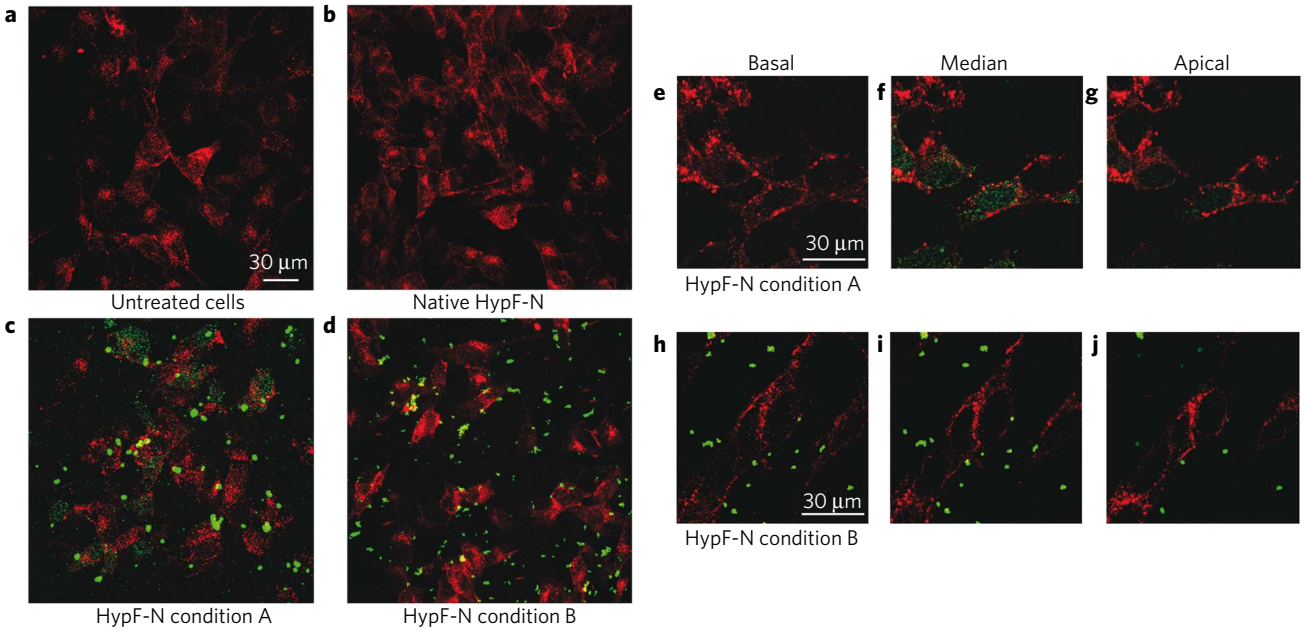

Figure 4 | Interaction of the aggregates formed under conditions A and B with cells. (**a**–**d**) Confocal scanning microscopy images of SH-SY5Y cells untreated (**a**) or treated with 12 µM native HypF-N (**b**), 12 µM HypF-N pre-incubated under condition A (**c**) and 12 µM HypF-N pre-incubated under condition B (**d**). (**e**–**j**) Optical sections taken through the cells after treatment with 12 µM HypF-N pre-incubated under conditions A (**e**–**g**) and B (**h**–**j**) at basal (**e**,**h**), median (**f**,**i**) and apical (**g**,**j**) focal lengths. In all images, red and green fluorescence indicates cell profiles and HypF-N, respectively.

ratios measured at given positions for the two types of aggregates are unlikely to be the result of an intrinsic ability of the fluorophore to affect the aggregation process, as this interference would be revealed in both sets of conditions at the same positions. The observation that the excimer ratio is higher for the species formed under condition A at only a small number of positions rules out the possibility that the ability of PM to perturb the oligomerization process is condition-dependent. Moreover, the low values of the excimer ratios at some positions indicate that PM does not intrinsically drive the formation of intermolecular interactions between PM moieties from different HypF-N molecules. As a further confirmation, fluorescence emission spectra acquired under both conditions with PM-labeled β-mercaptoethanol indicated that the PM moiety is intrinsically soluble under the experimental conditions used in the present study and does not *per se* drive the aggregation process (**Supplementary Fig. 6b**).

In order to check whether the oligomeric species formed in conditions A and B varied their structure upon transfer into a physiological buffer at neutral pH, in which the morphology and toxicity to cultured cells was assessed, samples of HypF-N labeled at positions 10, 25, 47, 59, 65 and 83 were separately incubated in both conditions A and B and analyzed before and after dilution into 20 mM potassium phosphate buffer, pH 7.0. For each sample, the resulting PM emission spectra were similar before and after change of solution conditions, ruling out the possibility of marked structural changes within the preformed aggregates (**Supplementary Fig. 7**).

In another control experiment, the effect of protein concentration on the excimer ratio values was also tested, indicating that the difference between toxic and nontoxic aggregates persists at all protein concentrations examined, including the lowest (**Supplementary Fig. 3c**). Finally, oligomers formed in condition B using 1:1 mixtures of labeled and unlabeled chains did not exhibit marked excimer ratio values, indicating that low values of the excimer ratio for the nontoxic oligomers are obtained only when the probability of two PM moieties being in close proximity is reduced (**Supplementary Fig. 3d**).

Toxic oligomers bind ANS more tightly

To have an independent probe of hydrophobic exposure in the two types of oligomers, we also tested the ability of the two species to interact with 8-anilinonaphthalene-1-sulfonate (ANS), a dye that has been shown to bind to solvent-exposed hydrophobic

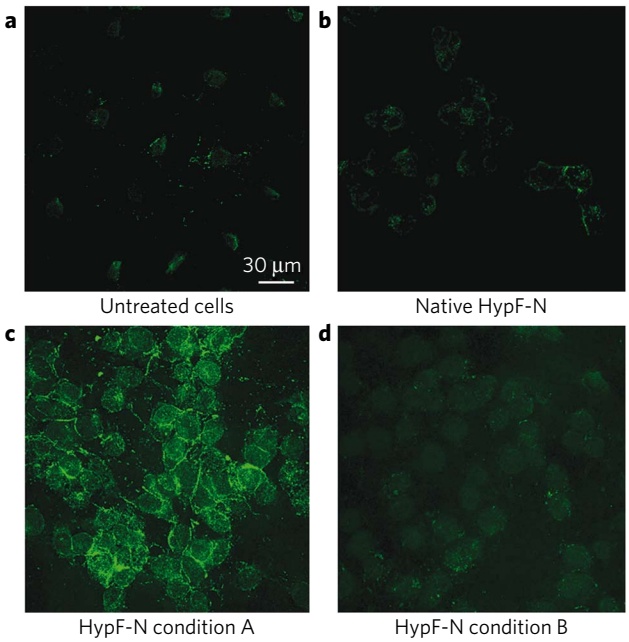

Figure 5 | Dysregulation of cytosolic Ca^{2+} by aggregates formed under conditions A and B. (**a**–**d**) Confocal scanning microscopy images of SH-SY5Y cells showing changes in intracellular free Ca^{2+} levels, when cells are untreated (**a**) or treated with 12 µM native HypF-N (**b**), 12 µM HypF-N pre-incubated under condition A (**c**) and 12 µM HypF-N pre-incubated under condition B (**d**). In all images, the green fluorescence arises from the intracellular Fluo3 probe bound to Ca^{2+}.

clusters, and thereby to generate a marked increase in its fluorescence emission intensity and a blue shift of its maximum emission wavelength[27,28]. At equivalent ANS concentrations, the fluorescence intensity measured in the presence of the toxic oligomers was higher than that obtained with nontoxic oligomers, indicating a higher degree of exposure to the solvent of hydrophobic clusters in the toxic species (**Fig. 3i**). Moreover, the wavelength of maximum emission (λ_{max}) was lower for the toxic oligomers than for the nontoxic species, indicating that the dye interacts with a more nonpolar environment (**Fig. 3i**). No significant ANS binding was detected for native HypF-N (**Supplementary Fig. 8**).

HypF-N oligomers differ in cell membrane interaction

It has repeatedly been reported that oligomers can interact with and permeabilize synthetic lipid vesicles[29] and cell membranes[14]. In order to assess whether or not the structural differences between the two types of oligomers detected with PM labeling and ANS binding are associated with differences in their interactions with the cell membrane, HypF-N aggregates formed under conditions A and B were added to SH-SY5Y cell culture media. The cells were then extensively washed and examined by confocal scanning microscopy and immunofluorescence using anti-HypF-N antibodies. Both toxic and nontoxic oligomers were found to bind to the treated cells; by contrast, control experiments carried out with the monomeric protein showed no interaction (**Fig. 4a–d**). Nevertheless, the imaging of different optical sections of the cells exposed to the oligomers, including basal, apical and intermediate median planes, revealed the presence of HypF-N aggregates inside the cells (median planes) only when these were treated with the toxic oligomers formed under condition A (**Fig. 4e–j**). The presence of only toxic oligomers inside the cells cannot be attributed to the different size of these species, as AFM images indicate that the two types of oligomers are submicroscopic and comparable in size (**Fig. 1a,b**). In addition, small green dots were detectable in confocal microscopy images outside the cells in both cases (**Supplementary Fig. 9**). These results indicate that only the toxic aggregates have sufficiently high structural plasticity and hydrophobic surface to penetrate the cell membrane and even cross it and reach the interior of the cell.

We then performed a confocal microscope analysis of the cytosolic Ca^{2+} content in SH-SY5Y cells upon exposure to HypF-N aggregates. Addition of the toxic oligomers formed under condition A to the cell culture media was found to cause a large influx of extracellular Ca^{2+} ions into the cytosol, much like the oligomers formed by other proteins and peptides[30]; by contrast, addition of the nontoxic oligomers formed under condition B did not cause any increase of intracellular Ca^{2+} ions, as observed upon exposure to the native protein (**Fig. 5**).

The ability of both types of oligomers to bind to cell membranes is consistent with the observation that both can bind to ANS, albeit with different efficiencies. However, the finding that only the toxic oligomers cross the hydrophobic bilayer of the cell membrane is consistent with the conclusions of the PM-labeling and ANS binding studies that the hydrophobic regions of the toxic oligomers are more structurally disorganized and solvent exposed than those of the nontoxic species.

DISCUSSION

It is well known that incubation of the same peptide or protein under different experimental conditions causes the formation of oligomers or fibrils with different morphologies and that such differences result in different degrees of toxicity[31–35]. Similarly, mutations or covalent modifications can result in different levels of oligomers or different fibrillar structures with completely different toxicities[36,37]. However, little experimental information is available on the structural features of oligomers grown under different conditions and on the relationship between their structure and their ability to cause cell dysfunction. In the present study, oligomers formed from the same protein under different conditions were found to exhibit similar morphological and tinctorial properties, yet they differ in their molecular structure and ability to cause cell dysfunction. Comparisons of the two types of aggregates described here indicate that their structural differences result from different degrees of packing of the hydrophobic residues within their cores, with toxicity associated with the level of structural flexibility and solvent-exposure of such residues. Furthermore, our results indicate that the toxicity is associated with the ability of the oligomeric species to form a more pronounced and disruptive interaction with the cells, stimulating Ca^{2+} influx and leading to cell death. Hence, whereas the ability to form amyloid-like structures is generic to polypeptide chains, whether or not such species are pathogenic depends on their structural features, notably the extent to which hydrophobic residues are flexible and exposed on their surfaces within the environment of a living organism.

Our ability to characterize these two forms of oligomers can be attributed to the high aggregation propensity of HypF-N, which has allowed oligomeric states that would normally be metastable to be trapped. Our findings, however, do not seem to be limited to the HypF-N aggregates, and could indeed explain the toxic properties of the oligomers formed by disease-related systems. Hydrogen/deuterium (H/D) exchange measurements carried out on the protofibrils and mature fibrils formed by the 40-residue form of the amyloid-β peptide ($A\beta_{40}$), the peptide associated with Alzheimer's disease, indicate that the degree of protection from H/D exchange, observed at the level of the two regions of the sequence forming the structural core of both types of aggregates, is higher in the fibrils than in the protofibrils[38]. Moreover, in the case of the fibrils, some of the residues flanking these two regions are also protected from H/D exchange[38]. Notably, these two regions correspond to the highest peaks in the hydropathy profile of this peptide, suggesting that the higher degree of structure of these hydrophobic portions of the sequence in the fibrils could explain why mature $A\beta_{40}$ fibrils are less toxic than protofibrils[6]. Other results also indicate a correlation between the size and surface hydrophobicity of $A\beta_{40}$ aggregates and their ability to decrease the bilayer fluidity of model membranes[39], suggesting that the exposure to the solvent of hydrophobic surfaces determines the ability of these species to interact with cell membranes. A correlation between hydrophobicity, tendency to form aggregates and aggregate cytotoxicity has also been observed in comparative studies where the behavior of different homopolymeric amino acid (HPAA) stretches was investigated[40,41].

It has been recently reported that expanded huntingtin-exon1 forms fibrillar aggregates at two different temperatures that have different structural and physical properties as well as different cytotoxicities[35]. The structures and toxicities of both forms of the aggregates are comparable with those extracted from regions of mouse brains affected to different extents by huntingtin deposition. In both pairs of structures, a direct relationship between structural flexibility and cytotoxicity of amyloid assemblies was found, supporting the generality of our conclusions[35].

In conclusion, the data obtained here lend support to the idea that a key feature in the generation of toxicity is the conversion of a species of aggregates in which stability is associated with extreme burial of hydrophobic residues to one in which such residues are substantially exposed and disorganized[42]. On the same grounds, we suggest that for therapeutic purposes the toxicity can be substantially reduced if the hydrophobic residues are incorporated to a greater extent within the interior of the oligomeric assemblies, even in the absence of an effective change in morphology. From a broader perspective, our data establish a link between biological activity of aberrant protein oligomers and precise structural features within them. They suggest that solvent-exposed and structurally disorganized hydrophobic residues within small protein oligomers are at the origin of the

pathogenesis of important debilitating human diseases and can represent important molecular targets for therapeutic intervention.

METHODS

Protein expression, purification and mutagenesis. Wild-type and mutated HypF-N production was carried out as described in **Supplementary Methods**. Purified proteins were stored at −20 °C in 5 mM acetate buffer, pH 5.5, with 2 mM dithiothreitol (DTT). Mutations in the gene coding for wild-type HypF-N were generated using the QuickChange site-directed mutagenesis kit (Stratagene), as described in **Supplementary Methods**. The molecular mass of the purified variants was checked with MALDI-MS. The protein purity was found by SDS-PAGE to be >95% in all cases. The purified variants were stored at −20 °C in 100 mM potassium phosphate buffer, pH 7.0, with 2 mM tris(2-carboxyethyl)phosphine hydrochloride.

Preparation of HypF-N oligomers. Oligomers were prepared by diluting the protein stock solution to 48 μM in (i) 50 mM acetate buffer, 12% (v/v) trifluoroethanol (TFE), 2 mM DTT, pH 5.5 (condition A) and (ii) 20 mM trifluoroacetic acid (TFA), 330 mM NaCl, pH 1.7 (condition B). The resulting samples were incubated for 4 h at 25 °C.

TM-AFM. Aggregates were centrifuged at 16,100 r.c.f. for 10 min and resuspended in potassium phosphate buffer, pH 7.0. 10 μl of each sample was diluted 100 times (or 500 times for samples not resuspended at pH 7.0), deposited on a freshly cleaved mica substrate and dried under vacuum. TM-AFM images were acquired in air using a Dimension 3100 SPM with a 'G' scanning head (maximum scan size 100 μm) and driven by a Nanoscope IIIa controller, and a Multimode SPM equipped with 'E' scanning head (maximum scan size 10 μm) and driven by a Nanoscope IV controller (Digital Instruments, Veeco). Single beam uncoated silicon cantilevers (type OMCL-AC160TS, Olympus) were used. The drive frequency was between 320 and 340 kHz; the scan rate was 0.5–2.0 Hz. Aggregate sizes were measured from the height in cross section of the topographic AFM images; due to the drying procedure applied, the measured heights were multiplied by a shrinking factor of 2.2 and evaluated comparing the heights of native HypF-N under liquid and after drying.

MTT assay and Hoeschst staining test. Human SH-SY5Y neuroblastoma cells and mouse Hend endothelium cells were cultured as described in **Supplementary Methods**. Both types of HypF-N aggregates were centrifuged at 16,100 r.c.f., dried under N_2 to remove TFE when necessary, dissolved in DMEM without phenol red and immediately added to the cell media of SH-SY5Y and Hend cells for 24 h, at 12 μM monomer concentration. Aggregates of $A\beta_{42}$ and IAPP (refs. 17,18) were tested at the same concentration. HypF-N aggregates formed under condition B were also tested at 2 and 48 μM. Native HypF-N was tested by diluting the stock solution of HypF-N to a final protein concentration of 12 μM. Cytotoxicity was assessed by the MTT assay as reported in **Supplementary Methods**. SH-SY5Y cells treated for 24 h with 12 μM of the aggregates formed by HypF-N, $A\beta_{42}$ and IAPP or 12 μM native HypF-N were stained with the Hoechst 33342 dye as described in **Supplementary Methods**.

Labeling with PM. Each protein variant was diluted to 0.2 mM in 100 mM potassium phosphate, pH 7.0, 3 M guanidine hydrochloride. Aliquots of PM (Molecular Probes) in DMSO were added to a tenfold molar excess of dye. The sample was left in the dark on a shaker for 1 h at 37 °C, then overnight at 4 °C. The reaction was quenched with 5 μl of trifluoroacetic acid. The unbound dye was removed by extensive dialysis (3.0 kDa cutoff), and the sample was centrifuged to remove any precipitate. The concentration of PM was determined using ε_{344nm} = 40,000 M^{-1} cm^{-1} (ref. 43). Protein concentration was measured at 280 nm after subtraction of the contribution of PM.

Pyrene fluorescence emission spectra. Fluorescence emission spectra of the type A and B PM-labeled aggregates were measured at 25 °C on a PerkinElmer LS 55 spectrofluorimeter with an excitation of 344 nm. Protein concentration was 48 μM. The spectra were smoothed and normalized to the intensity of the peak at 375 nm.

ANS titration. Both types of HypF-N aggregates formed at 48 μM were centrifuged for 10 min at 16,100 r.c.f. The pellets were resuspended in 20 mM potassium phosphate buffer, pH 7.0. Aliquots of ANS from a stock solution in 20 mM potassium phosphate buffer, pH 7.0, were subsequently added to the aggregates, to a final ANS concentration ranging from 0 to 237 μM. The final protein concentration was 43 μM in all cases. The spectra were immediately acquired and processed as described in **Supplementary Methods**. The difference between the resulting fluorescence intensity at 470 nm and that measured with only protein in the absence of ANS was used as the effective ANS fluorescence.

Interaction of the aggregates with the cell membrane. SH-SY5Y cells were seeded on glass coverslips and analyzed using a Leica TCS SP5 confocal scanning microscope, equipped with an argon laser source. Cells were first treated for 60 min at 37 °C with native HypF-N or with aggregates formed under conditions A and B, after centrifugation at 16,100 r.c.f. and resuspension of the pellet in DMEM without phenol red. The final protein concentration was 12 μM. The cells were washed with phosphate-buffered saline, counterstained for 10 min with 50 μg ml^{-1} Alexa Fluor 633–conjugated wheat germ agglutinin and fixed in 2% (w/v) buffered paraformaldehyde for 10 min at room temperature (20 °C). After plasma membrane permeabilization with a 3% (v/v) glycerol solution for 5 min, the coverslips were incubated for 60 min with 1:1,000 diluted rabbit polyclonal anti-HypF-N antibodies (Primm srl) and then for 90 min with 1:1,000 diluted Alexa Fluor 488–conjugated anti-rabbit secondary antibodies.

Cytosolic Ca^{2+} dysregulation. SH-SY5Y cells seeded on glass coverslips were treated with native HypF-N or aggregates as described above. Cells were then washed and loaded for 30 min at 37 °C with 10 μM Fluo3-AM, 0.01% (w/v) pluronic acid F-127 in Hank's Balanced Salt Solution. Cells were then washed and fixed in 2.0% (w/v) buffered paraformaldehyde for 10 min at room temperature. The analysis was performed using the confocal scanning system described above.

Accession codes. Protein Data Bank: The native structure of HypF-N was deposited as part of a previous study under accession code 1GXU.

Received 24 September 2009; accepted 6 November 2009; published online 10 January 2010

References

1. Chiti, F. & Dobson, C.M. Protein misfolding, functional amyloid, and human disease. *Annu. Rev. Biochem.* **75**, 333–366 (2006).
2. Janson, J., Ashley, R.H., Harrison, D., McIntyre, S. & Butler, P.C. The mechanism of islet amyloid polypeptide toxicity is membrane disruption by intermediate-sized toxic amyloid particles. *Diabetes* **48**, 491–498 (1999).
3. Sousa, M.M. & Saraiva, M.J. Neurodegeneration in familial amyloid polyneuropathy: from pathology to molecular signaling. *Prog. Neurobiol.* **71**, 385–400 (2003).
4. Merlini, G. & Bellotti, V. Molecular mechanisms of amyloidosis. *N. Engl. J. Med.* **349**, 583–596 (2003).
5. Silveira, J.R. *et al.* The most infectious prion protein particles. *Nature* **437**, 257–261 (2005).
6. Rahimi, F., Shanmugam, A. & Bitan, G. Structure-function relationships of pre-fibrillar protein assemblies in Alzheimer's disease and related disorders. *Curr. Alzheimer Res.* **5**, 319–341 (2008).
7. Cookson, M.R. & van der Brug, M. Cell systems and the toxic mechanism(s) of alpha-synuclein. *Exp. Neurol.* **209**, 5–11 (2008).
8. Kayed, R. *et al.* Common structure of soluble amyloid oligomers implies common mechanism of pathogenesis. *Science* **300**, 486–489 (2003).
9. Rosano, C. *et al.* Crystal structure and anion binding in the prokaryotic hydrogenase maturation factor HypF acylphosphatase-like domain. *J. Mol. Biol.* **321**, 785–796 (2002).
10. Chiti, F. *et al.* Solution conditions can promote formation of either amyloid protofilaments or mature fibrils from the HypF N-terminal domain. *Protein Sci.* **10**, 2541–2547 (2001).
11. Marcon, G. *et al.* Amyloid formation from HypF-N under conditions in which the protein is initially in its native state. *J. Mol. Biol.* **347**, 323–335 (2005).
12. Campioni, S. *et al.* Conformational properties of the aggregation precursor state of HypF-N. *J. Mol. Biol.* **379**, 554–567 (2008).
13. Bucciantini, M. *et al.* Inherent toxicity of aggregates implies a common mechanism for protein misfolding diseases. *Nature* **416**, 507–511 (2002).
14. Bucciantini, M. *et al.* Prefibrillar amyloid protein aggregates share common features of cytotoxicity. *J. Biol. Chem.* **279**, 31374–31382 (2004).
15. Baglioni, S. *et al.* Prefibrillar amyloid aggregates could be generic toxins in higher organisms. *J. Neurosci.* **26**, 8160–8167 (2006).
16. Mosmann, T. Rapid colorimetric assay for cellular growth and survival: application to proliferation and cytotoxicity assays. *J. Immunol. Methods* **65**, 55–63 (1983).
17. Cecchi, C. *et al.* Seladin-1/DHCR24 protects neuroblastoma cells against Abeta toxicity by increasing membrane cholesterol content. *J. Cell. Mol. Med.* **12**, 1990–2002 (2008).
18. Cecchi, C. *et al.* Replicating neuroblastoma cells in different cell cycle phases display different vulnerability to amyloid toxicity. *J. Mol. Med.* **86**, 197–209 (2008).
19. Downs, T.R. & Wilfinger, W.W. Fluorometric quantification of DNA in cells and tissue. *Anal. Biochem.* **131**, 538–547 (1983).
20. Birks, J.B. Excimers and exciplexes. *Nature* **214**, 1187–1190 (1967).
21. Hammarström, P. *et al.* Structural mapping of an aggregation nucleation site in a molten globule intermediate. *J. Biol. Chem.* **274**, 32897–32903 (1999).
22. Krishnan, R. & Lindquist, S.L. Structural insights into a yeast prion illuminate nucleation and strain diversity. *Nature* **435**, 765–772 (2005).
23. Dong, D.C. & Winnik, M.A. The Py scale of solvent polarities. *Can. J. Chem.* **62**, 2560–2565 (1984).

24. Christensen, P.A., Pedersen, J.S., Christiansen, G. & Otzen, D.E. Spectroscopic evidence for the existence of an obligate pre-fibrillar oligomer during glucagon fibrillation. *FEBS Lett.* **582**, 1341–1345 (2008).
25. Hammarström, P. *et al.* Structural mapping of an aggregation nucleation site in a molten globule intermediate. *J. Biol. Chem.* **274**, 32897–32903 (1999).
26. Thirunavukkuarasu, S., Jares-Erijman, E.A. & Jovin, T.M. Multiparametric fluorescence detection of early stages in the amyloid protein aggregation of pyrene-labeled alpha-synuclein. *J. Mol. Biol.* **378**, 1064–1073 (2008).
27. Semisotnov, G.V. *et al.* Study of the "molten globule" intermediate state in protein folding by a hydrophobic fluorescent probe. *Biopolymers* **31**, 119–128 (1991).
28. Cardamone, M. & Puri, N.K. Spectrofluorimetric assessment of the surface hydrophobicity of proteins. *Biochem. J.* **282**, 589–593 (1992).
29. Kayed, R. *et al.* Permeabilization of lipid bilayers is a common conformation-dependent activity of soluble amyloid oligomers in protein misfolding diseases. *J. Biol. Chem.* **279**, 46363–46366 (2004).
30. Demuro, A. *et al.* Calcium dysregulation and membrane disruption as a ubiquitous neurotoxic mechanism of soluble amyloid oligomers. *J. Biol. Chem.* **280**, 17294–17300 (2005).
31. Petkova, A.T. *et al.* Self-propagating, molecular-level polymorphism in Alzheimer's beta-amyloid fibrils. *Science* **307**, 262–265 (2005).
32. Inaba, S., Okada, T., Konakahara, T. & Kodaka, M. Specific binding of amyloid-beta-protein to IMR-32 neuroblastoma cell membrane. *J. Pept. Res.* **65**, 485–490 (2005).
33. Lee, S., Fernandez, E.J. & Good, T.A. Role of aggregation conditions in structure, stability, and toxicity of intermediates in the Abeta fibril formation pathway. *Protein Sci.* **16**, 723–732 (2007).
34. Kayed, R. *et al.* Annular protofibrils are a structurally and functionally distinct type of amyloid oligomer. *J. Biol. Chem.* **284**, 4230–4237 (2009).
35. Nekooki-Machida, Y. *et al.* Distinct conformations of *in vitro* and *in vivo* amyloids of huntingtin-exon1 show different cytotoxicity. *Proc. Natl. Acad. Sci. USA* **106**, 9679–9684 (2009).
36. Yoshiike, Y., Akagi, T. & Takashima, A. Surface structure of amyloid-beta fibrils contributes to cytotoxicity. *Biochemistry* **46**, 9805–9812 (2007).
37. Hung, L.W. *et al.* Amyloid-beta peptide (Abeta) neurotoxicity is modulated by the rate of peptide aggregation: Abeta dimers and trimers correlate with neurotoxicity. *J. Neurosci.* **28**, 11950–11958 (2008).
38. Kheterpal, I. & Wetzel, R. Hydrogen/deuterium exchange mass spectrometry—a window into amyloid structure. *Acc. Chem. Res.* **39**, 584–593 (2006).
39. Kremer, J.J., Pallitto, M.M., Sklansky, D.J. & Murphy, R.M. Correlation of β-amyloid aggregate size and hydrophobicity with decreased bilayer fluidity of model membranes. *Biochemistry* **39**, 10309–10318 (2000).
40. Oma, Y., Kino, Y., Sasagawa, N. & Ishiura, S. Intracellular localization of homopolymeric amino acid-containing proteinexpressed in mammalian cells. *J. Biol. Chem.* **279**, 21217–21222 (2004).
41. Oma, Y., Kino, Y., Sasagawa, N. & Ishiura, S. Comparative analysis of the cytotoxicity of homopolymeric amino acids. *Biochim. Biophys. Acta* **1748**, 174–179 (2005).
42. Cheon, M. *et al.* Structural reorganisation and potential toxicity of oligomeric species formed during the assembly of amyloid fibrils. *PLoS Comput. Biol.* **3**, 1727–1738 (2007).
43. Haugland, R.P. Thiol-reactive probes excited with ultraviolet light. in *Handbook of Fluorescent Probes and Research Products* 9th edn. (ed. Gregory, J.) 95 (Molecular Probes, Eugene, Oregon, USA, 2002).
44. Roseman, M.A. Hydrophilicity of polar amino acid side-chains is markedly reduced by flanking peptide bonds. *J. Mol. Biol.* **200**, 513–522 (1988).
45. Koradi, R., Billeter, M. & Wüthrich, K. MOLMOL: a program for display and analysis of macromolecular structures. *J. Mol. Graph.* **14**, 51–55 (1996).

Acknowledgments

This work was supported by the European Union (Project EURAMY), by the Italian Ministero dell'Istruzione, Università e Ricerca (FIRB RBNE03PX83, PRIN 2006058958 and PRIN 2007XY59Z), Fondazione Cariplo, Ente Cassa di Risparmio di Firenze (project "Lipid rafts" 2008) and the European Molecular Biology Organization Young Investigator Programme. We are grateful to S. Torrassa and D. Nichino for assistance with AFM measurements and to I. Shalova for assistance in the purification and labeling of some of the variants used in this work.

Author contributions

S.C. and F.C. designed the variants and the experiments to investigate the structure of HypF-N oligomers. S.C. (in part also B.M.) produced, purified and labeled all the variants and performed all the fluorescence experiments (PM, ThT and ANS). A.P. and E.E. performed the MTT assays. M.Z. performed the confocal microscopy experiments. C.P. and A.R. designed, performed and analyzed the AFM data. M.S. and C.C. supervised the experiments on cell cultures. F.C. supervised all the experiments. S.C., C.M.D. and F.C. wrote the manuscript with contributions from A.R., C.C. and M.S.

Additional information

Supplementary information is available online at http://www.nature.com/naturechemicalbiology/. Reprints and permissions information is available online at http://npg.nature.com/reprintsandpermissions/. Correspondence and requests for materials should be addressed to F.C.